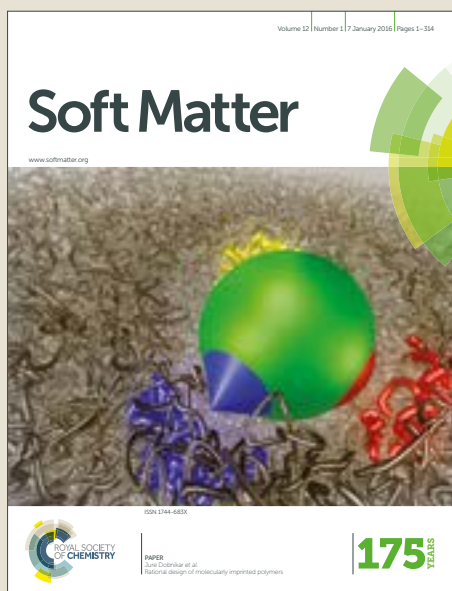


Soft Matter

Accepted Manuscript



This article can be cited before page numbers have been issued, to do this please use: J. Puig, M. Ceolín, R. Williams, W. F. Schroeder and I. A. zucchini, *Soft Matter*, 2017, DOI: 10.1039/C7SM01660C.



This is an Accepted Manuscript, which has been through the Royal Society of Chemistry peer review process and has been accepted for publication.

Accepted Manuscripts are published online shortly after acceptance, before technical editing, formatting and proof reading. Using this free service, authors can make their results available to the community, in citable form, before we publish the edited article. We will replace this Accepted Manuscript with the edited and formatted Advance Article as soon as it is available.

You can find more information about Accepted Manuscripts in the [author guidelines](#).

Please note that technical editing may introduce minor changes to the text and/or graphics, which may alter content. The journal's standard [Terms & Conditions](#) and the ethical guidelines, outlined in our [author and reviewer resource centre](#), still apply. In no event shall the Royal Society of Chemistry be held responsible for any errors or omissions in this Accepted Manuscript or any consequences arising from the use of any information it contains.

Controlling the generation of bilayer and multilayer vesicles in block copolymer / epoxy blends by a slow photopolymerization process

J. Puig,^a M. Ceolín,^b R. J. J. Williams,^a W. F. Schroeder,^a and I. A. Zucchi^{a,*}

^a *Institute of Materials Science and Technology (INTEMA), University of Mar del Plata and National Research Council (CONICET), J. B. Justo 4302, B7608FDQ, Mar del Plata, Argentina.*

^b *Instituto de Investigaciones Fisicoquímicas Teóricas y Aplicadas (INIFTA), Universidad Nacional de La Plata, CONICET, CC 16-Suc. 4, La Plata, Argentina*

*to whom correspondence should be addressed

ABSTRACT

Vesicles are a highly attractive morphology to achieve in micellar dispersions of block copolymers (BCP) in epoxy thermosets due to the fact that small amounts can affect a large volume fraction of the matrix, a fact that is important for toughening purposes. However, generating vesicles in epoxy matrices requires operating in a narrow range of formulations and processing conditions. In this report we show that block-copolymer vesicles dispersed in an epoxy matrix could be obtained through a sphere-to-cylinder-to-vesicle micellar transition induced by visible-light photopolymerization at room temperature. A 10 wt% colloidal solution of poly(ethylene-*co*-butene)-*block*-poly(ethylene oxide) (PEB-*b*-PEO) block copolymer (BCP) in an epoxy monomer (DGEBA), self-assembled into spherical micelles as shown by small-angle X-ray scattering (SAXS). During a slow photopolymerization of the epoxy monomer carried out at room temperature, a sphere-to-cylinder-to-vesicle transition took place as revealed by *in situ* SAXS and TEM images. This was driven by the tendency of the system to reduce the local interfacial curvature as a response to a decrease of the miscibility of PEO blocks in the polymerizing epoxy matrix. When the BCP concentration was increased from 10 to 20 and 40 wt%, the final structure evolved from bilayer vesicles to multilayer vesicles and to lamellae, respectively. In particular, for 20 wt% PEB-*b*-PEO, transient structures such as partially fused multilayered vesicles were observed by TEM, giving insight into the growth mechanism of multilayer vesicles. On the contrary, when a relatively fast thermal polymerization was performed at 80 °C, the final morphology consisted of kinetically-trapped spherical micelles. Hopefully, this study will lead to new protocols for the preparation of vesicles dispersed in epoxy matrices in a controlled way.

1. INTRODUCTION

Amphiphilic block copolymers (BCP) can self-assemble in a selective solvent to form a range of micellar morphologies, such as spheres, cylinders, vesicles, lamellae, and many other hierarchical assemblies.^{1,2} Increasing the amount of BCP in the solution, ordered phases such as body-centered cubic packed spheres, hexagonally packed cylinders, gyroid, and lamellae can be formed.¹ In any case, the developed morphology is governed by a balance of contributions to the free energy, involving the interfacial energy between the micellar core and the solvent, the stretching of the core forming blocks, and the repulsive interactions among corona chains.³ Therefore, morphologies can be controlled by a number of factors, such as molecular weight, composition and concentration of the BCP, block–block and block–solvent interaction parameters, and the properties of the solvent.^{4–6}

Among the various micellar morphologies, vesicles are of special interest because of their promising applications in areas such as drug delivery,⁷ magnetic resonance imaging and theranostics,^{7,8} cell mimicking,^{9–11} nano-reactors,^{9,12} perfume containers,¹³ catalysis,^{12,14} water remediation^{12,15} and even construction materials.¹⁶ In particular, vesicles are a highly attractive morphology to be developed in nanostructured epoxy thermosets. Vesicles are spherical objects formed by a thin bilayer membrane (ca. 10 nm) that encloses the epoxy matrix. The interest in this morphology resides on the fact that the copolymer forms only the shell (a thin bilayer membrane) whereas the volume of the vesicle phase consists of the shell plus the portion of encapsulated epoxy matrix. Therefore, a small amount of BCP can modify a large effective volume of the matrix. Due to this feature, vesicles have been found to be interesting nanostructures for epoxy toughening. However, the toughening effect of vesicles varies significantly among different epoxy systems.^{4,17–21}

Traditionally, BCP vesicles in solution have been obtained via a two-step approach (so-called *solvent displacement method*). First, the copolymer chains are molecularly dissolved in a good solvent for both blocks, and then solvency for one of the blocks is reduced to drive microphase separation. For example, Luo and Eisenberg²² dissolved poly(styrene)-*block*-poly(acrylic acid) (PS-*b*-PAA) diblock copolymers in a THF/dioxane mixture and then gradually added water (a non-solvent for PS) to induce the formation of micellar aggregates. They demonstrated that at a critical water concentration, unimeric polymer chains present in solution aggregated into spherical micelles. As more water was added, the morphology of the aggregates was transformed from spheres to rods and then to vesicles, driven by the tendency to reduce the free energy of the system.

Recently, the Armes's group has obtained BCP vesicles in solution through an alternative route known as polymerization-induced self-assembly (PISA).²³ In this approach, a homopolymer initially dissolved in a suitable solvent is chain-extended with a second monomer through a controlled/living polymerization technique, commonly reversible addition-fragmentation chain transfer (RAFT) polymerization. Under such conditions, the growing second block becomes gradually insoluble, which induces *in situ* self-assembly to form BCP micelles. They reported formulations based on poly(2-hydroxypropyl methacrylate) (PHPMA) as the hydrophobic core-forming block and either poly(2-methacryloyloxy)ethyl phosphorylcholine (PMPC)²⁴ or poly(glycerol monomethacrylate) (PGMA)^{25,26} as the hydrophilic stabilizer block. It was demonstrated that if a relatively short stabilizer block is used, a morphological transformation from spheres to worms and then to vesicles can be observed, which is driven by the reduction in the free energy of the system as the core-forming PHPMA block grows.²³ The same

transformation was also observed by light-mediated polymerization-induced self-assembly.^{27,28}

Few studies have been reported on nanostructured epoxy networks modified with BCP vesicles.^{4,18–21,29–33} In most cases, vesicular aggregates were formed in the thermoset precursors before curing reaction, and then these were frozen by subsequent formation of the epoxy network. It was demonstrated that, under such conditions, vesicles can only be obtained within a very narrow concentration window. There are also several recent reports about polymerization induced self-assembly of BCP in epoxy matrices.^{34,35,36,37} In these cases, both blocks were miscible with the initial thermoset precursors, but one of them phase separated during polymerization while the other one remained miscible with the epoxy matrix. Various nanostructures in epoxy thermosets have been obtained by this way, such as cylindrical and spherical micelles,^{34,36} branched wormlike micelles,³⁶ multilamellar nanophases, and vesicles.³⁷ Based on the methods used to prepare vesicles in solution described above, we propose an alternative way to produce BCP vesicles in an epoxy matrix through a morphological transition from spheres to cylinders and then to vesicles induced by polymerization of the matrix. As it is well-known, the quality of the thermoset as a solvent of the corona-forming blocks varies with conversion.³⁸ Along polymerization, it changes from a good solvent to a poor one due to the increase in the average size before gelation (reduction in the entropic contribution to the free energy of mixing) and the increase in the crosslinking density after gelation. Therefore, under certain conditions, a sphere-to-cylinder-to-vesicle transition during epoxy polymerization should occur driven by the tendency of the system to reduce the local interfacial curvature and so the total free energy. In this case, unlike the methods used to prepare vesicles in solution described above, the morphology would be controlled by the degree of polymerization of the matrix.

In this study the possibility of capturing such a morphological transition during polymerization of an epoxy matrix based on diglycidyl ether of bisphenol A (DGEBA) was explored. The selected BCP was poly(ethylene-*co*-butene)-*block*-poly(ethylene oxide) (PEB-*b*-PEO) which self-assembles in DGEBA monomer into spherical micelles with PEB core and PEO shell. *In-situ* SAXS studies were conducted to monitor the morphology of the system as a function of epoxy conversion. The effect of both curing temperature and BCP concentration was investigated with the aim of finding a suitable protocol to obtain bilayer and multilayer vesicles in a controlled way.

2. EXPERIMENTAL SECTION

2.1. Materials. The selected BCP was poly(ethylene-*co*-butene)-*block*-poly(ethylene oxide) (PEB-*b*-PEO, Polymer Source, $M_n = 2700$, PDI = 1.09, 55 % addition 1,2 butadiene, 55 wt% ethylene oxide content). DSC analysis of the neat BCP indicated that PEB is an amorphous block while PEO exhibits characteristic melting and crystallization peaks, as shown in the Supporting Information (Figure S-1). A diglycidyl ether of bisphenol A monomer (DGEBA, DER 332 Aldrich Chemical Co.) with an epoxy equivalent weight of 174.3 g/eq was selected. The average number of hydroxyl groups per mol of DGEBA was 0.03. Benzyldimethylamine (BDMA, $\geq 99\%$) and camphorquinone (CQ) were purchased from Aldrich Chem. Co. p-(octyloxyphenyl) phenyliodonium hexafluoroantimonate (Ph_2ISbF_6) was supplied by Gelest Inc. (Philadelphia, USA). All materials were used as received. Chemical structures of these materials are shown in Figure 1.

2.2. Sample Preparation. PEB-*b*-PEO was blended with DGEBA in proper amounts to prepare blends containing 0, 1, 10, 20 and 40 wt% BCP. The mixtures were activated for visible light irradiation by the addition of a photoinitiating system based on two

components: Ph_2ISbF_6 (2 wt%) and CQ (1 wt%).^{39–41} The preparation of the samples was as follows: the total amount of BCP was blended with one-half of the total mass of DGEBA monomer. This mixture was first nitrogen purged for 30 min at room temperature, and then heated and stirred in an oil bath at 150 °C to disperse the PEB-*b*-PEO in the epoxy resin. The sample was removed from the oil bath and allowed to cool to room temperature. Then, the two components of the photoinitiating system dissolved in the remaining DGEBA were added. The resulting blend was nitrogen purged at room temperature for other 15 min, and then stirred and heated in the oil bath at 150 °C until a homogeneous mixture was obtained. Immediately after, the sample was cast onto an aluminum substrate (to obtain a film of ca. 1 mm thickness) or transferred to the apparatus used for its characterization.

The obtained films were photocured at room temperature with a light-emitting diode (LED) array in a circular configuration (Irradiance $I = 140 \text{ mW/cm}^2$ in the wavelength range between 410-530 nm). Under these conditions for hours of irradiation were required to attain morphologies that were not significantly changed by a further increase in conversion.

Also a blend containing 10 wt % PEB-*b*-PEO in DGEBA was thermally cured at 80 °C. Proper amounts of BCP and DGEBA were placed in a vial, purged with N_2 for 30 min at room temperature, and then immersed in an oil bath at 150 °C under continuous stirring until an homogeneous mixture was obtained.⁴² After cooling to room temperature, BDMA was added in a molar ratio with respect to epoxy groups equal to 0.06.⁴³ Then, the mixture was heated to 100 °C and stirred for about 1 min until the BDMA was correctly mixed. The resulting blend was transferred to the device used for characterization or cast onto an aluminum substrate (film of ca. 1 mm thickness). Cure was performed in a furnace under a N_2 atmosphere, at 80 °C for 4 h.

2.3. Characterization Techniques. *Fourier Transform Infrared Spectroscopy (FTIR).*

Near-Infrared Spectroscopy (NIR) was used to follow the conversion of epoxy groups. Spectra were acquired over the range 4000-7000 cm^{-1} from 32 co-added scans at 4 cm^{-1} resolution. The measurements were conducted on a Nicolet 6700 Thermo Scientific device. The sample was placed between glass windows using a 1.4 mm-rubber spacer. Photocurable samples were irradiated using the LED array and spectra were collected at different exposure times. For thermal curing, the device was provided with a heated transmission cell (HT-32, Spectra Tech) and a temperature controller (CAL 9500P, Spectra Tech). In both cases, the conversion of epoxy groups was followed by measuring the height of the absorption band at 4530 cm^{-1} (assigned to the conjugated epoxy CH_2 deformation band with the aromatic CH fundamental stretch) with respect to the height of a reference band at 4621 cm^{-1} (assigned to a combination band of the aromatic conjugated C=C stretch with aromatic CH fundamental stretch).⁴⁴

Small-Angle X-ray Scattering (SAXS). Experiments were performed *in situ* during both photocure at room temperature and thermal cure at 80 °C. SAXS diagrams of cured blends containing 1, 20 and 40 wt% BCP were also recorded at room temperature. The SAXS measurements were conducted in a XEUS 1.0 HR (XENOCs, Grenoble) apparatus equipped with a Pilatus 100K detector (Dectris, Switzerland) and a microfocus X-ray source, using $\lambda = 1.5419 \text{ \AA}$ wavelength radiation. For *in situ* experiments, the reactive blends were placed inside glass capillaries (borosilicate) with a thickness of 0.01 mm (Hampton Research) and an external diameter of 1.5 mm. The capillary was placed in a holder mounted in the X-ray beam path so that all SAXS diagrams were recorded at the same position with an acquisition time of 10 min. For photocuring samples, the LED array was concentrically located to the X-ray beam and SAXS curves were acquired at room temperature. For thermal cure, the sample

temperature was controlled using a HFSX350 device within ± 0.1 K (Linkam Scientific Instruments, UK). SASfit software package was used to analyze the scattering profiles.

Transmission Electron Microscopy (TEM). TEM micrographs were obtained by a JEOL 100CX electron microscope operated at 80 kV. Cured samples were ultrasectioned at room temperature by using an LKB ultramicrotome. Samples were stained with RuO_4 to enhance contrast between phases. RuO_4 selectively stains $\text{PEO} > \text{epoxy} > \text{PEB}$, from most stained to least stained.⁴⁵ The size distribution of nano-objects, their average size and the standard deviation, were determined using several images and employing more than 100 particles per image.

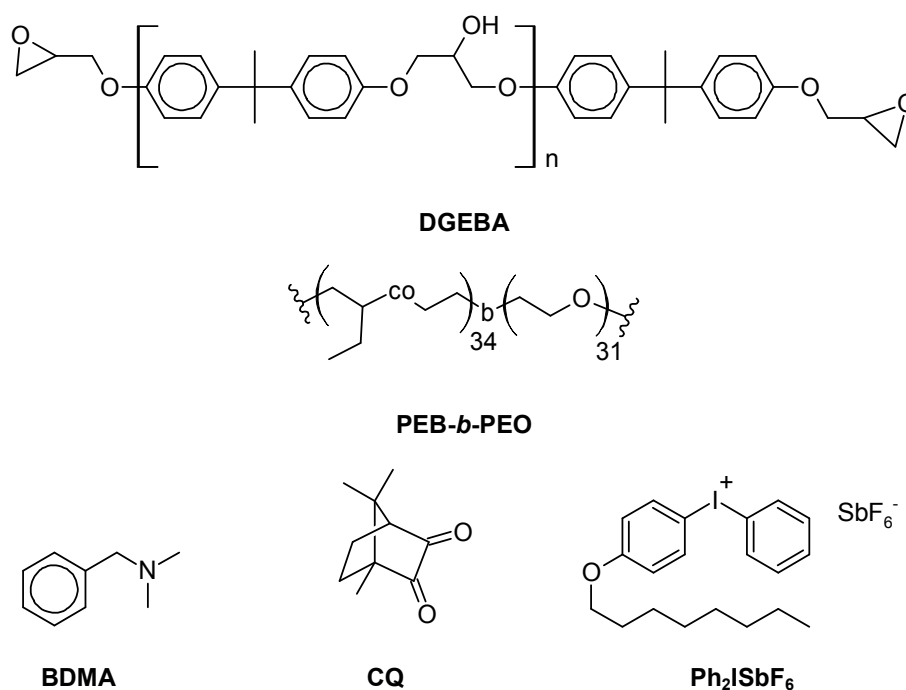


Figure 1. Chemical structures of the different materials.

3. RESULTS AND DISCUSSION

3.1. Blend with 10 wt% PEB-*b*-PEO

3.1.1. Curing at room temperature. We begin by examining a sample of DGEBA containing 10 wt% PEB-*b*-PEO cured at room temperature by visible-light cationic photopolymerization. The initiating mechanism has been previously discussed in the literature.^{46,47,48} Visible-light irradiation produces the excitation of CQ to its singlet, and then it is transferred to its triplet by intersystem crossing. Interaction of excited CQ with a hydrogen donor (monomers or trace impurities) produces ketyl radicals, which in turn are oxidized by the diaryliodonium salt to give rise to cationic species capable of initiating the polymerization of DGEBA.

The progress of the polymerization was monitored by following the decrease of the absorption band of epoxy groups at 4530 cm⁻¹ with respect to a reference band located at 4620 cm⁻¹.⁴⁹ Figure 2 shows conversion vs. time curves for the neat epoxy and for the blend with 10 wt% BCP. As can be observed, the addition of BCP decreased the polymerization rate of epoxy and increased the vitrification conversion (0.62) regarding to the neat epoxy sample (0.50). This result can be explained from the contribution of different effects. The miscibility of the PEO blocks with DGEBA produces, on the one hand, a dilution effect that decreases the polymerization rate, and on the other hand, a plasticization effect that displaces the T_g of the epoxy network to lower temperatures allowing to attain a higher vitrification conversion. In addition, effects associated to the cationic polymerization mechanism of DGEBA could also account for the obtained results. The PEO block has a hydroxyl chain end, and its hydrophilic character favors that water molecules can be initially introduced, compared to the neat epoxy sample. It is well known that hydroxyl containing compounds and water molecules can react with oxonium ion intermediates via the so-called Activated

Monomer (AM) mechanism.⁵⁰ As a result of this mechanism, an increase in the flexibility of the epoxy network is produced because of the formation of ether flexible links, which shifts the T_g of the network towards lower temperatures increasing the vitrification conversion. Another effect to be taken into account is that the PEO block could stabilize the oxonium intermediates by complexation, which would lead to a decrease in the rate of polymerization. Therefore, the conversion vs. time curve for the blend with BCP shown in Figure 2 should result from the contribution of all these effects. It is good to clarify that tack-free films were obtained after 4 h of irradiation in both cases.

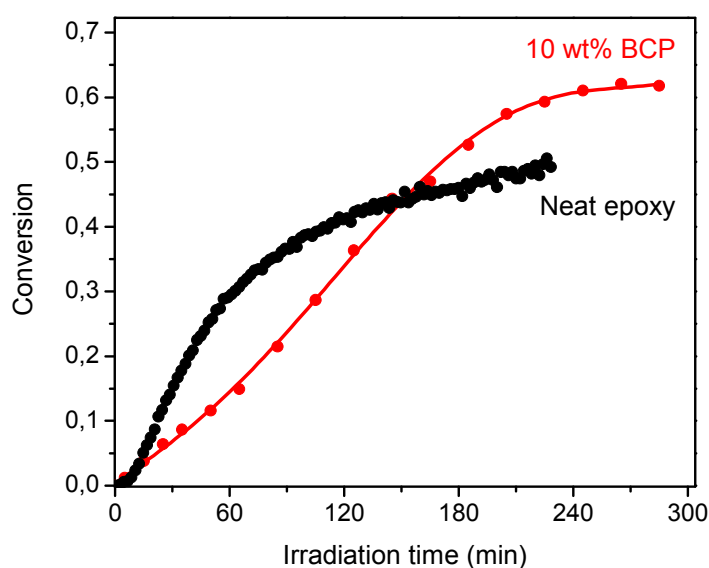


Figure 2. Conversion of epoxy groups as a function of irradiation time for blends containing 0 and 10 wt % PEB-*b*-PEO photocured at room temperature. Line is drawn to guide the eye.

The morphology of the epoxy thermoset with 10 wt % BCP obtained by photopolymerization at room temperature was characterized by transmission electron microscopy (TEM) and small-angle X-ray scattering (SAXS). After 4 h irradiation, vesicles dispersed in the epoxy matrix were observed. Figure 3 shows selected TEM

micrographs, with different degree of magnification, of a photo-cured sample stained with RuO₄. PEO-rich regions look darker in the TEM image as PEO blocks are preferentially stained by RuO₄ (compared to PEB blocks and epoxy matrix).⁴⁵ Bilayer vesicles are clearly distinguished in Figure 3. Furthermore, the staining technique allows distinguishing the location of the blocks in the structure. The TEM image at higher magnification (Fig. 3b) clearly shows vesicular structures exhibiting the epoxy-philic PEO corona as darker lines surrounding the epoxy-phobic PEB core (lighter line). The mean diameter of the vesicles was 78.6 ± 27.7 nm (see histogram in the inset to Fig. 3a).

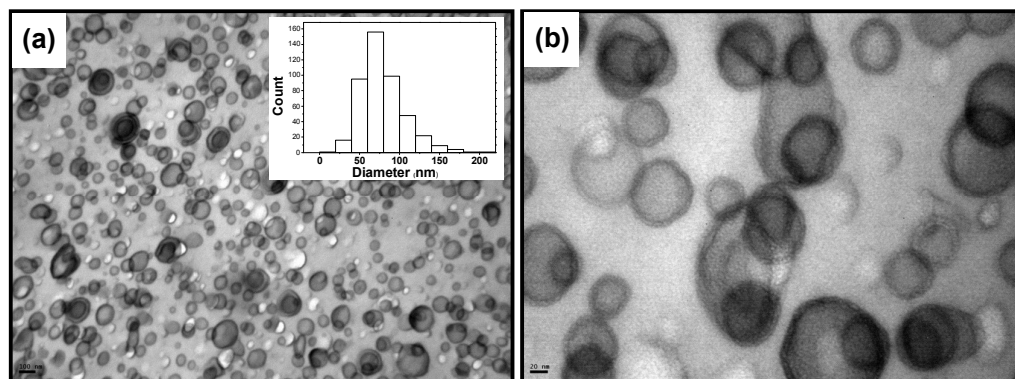
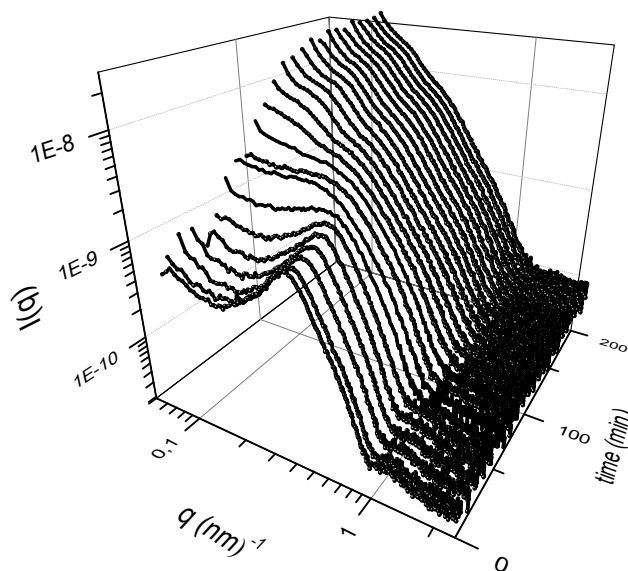


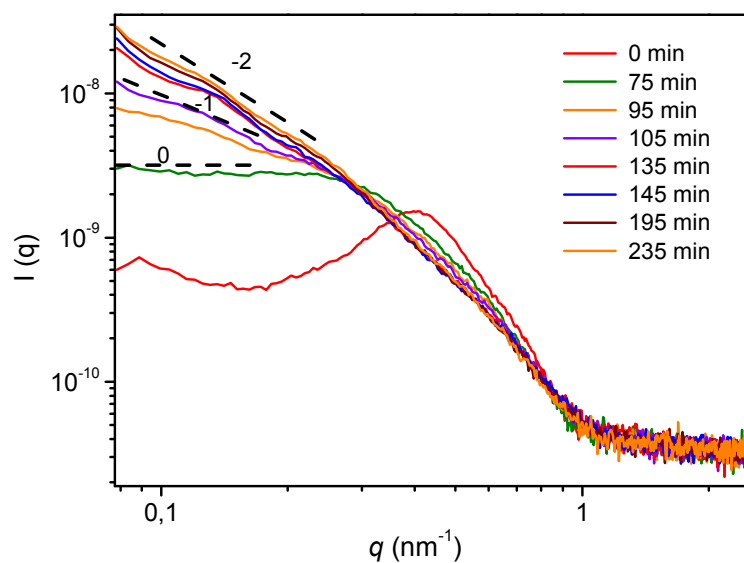
Figure 3. TEM images of the epoxy thermoset containing 10 wt % PEB-*b*-PEO. The specimen was stained with RuO₄ prior to the TEM observation. (a) Lower magnification, the black bar represents 100 nm, and (b) higher magnification, the black bar represents 20 nm.

Few studies have been reported on nanostructured epoxy networks modified with BCP vesicles.^{4,18–21,29–33} In all these cases, vesicular aggregates were formed in the thermoset precursors before curing reaction, and then these were frozen by subsequent formation of the epoxy network. To investigate if the resulting vesicles were already present in the initial blend or they formed during reaction, *in situ* SAXS measurements were performed. Figure 4 shows the SAXS curves as a function of irradiation time for the blend containing 10 wt % BCP.

In Figure 4a, a continuous change in the SAXS pattern with the reaction time is observed, indicating that the vesicular structure was the result of a polymerization-induced morphological transition (rather than a frozen-in morphology). Information about the evolution of the micellar structure as a function of irradiation time was obtained from the low- q region (Guinier regime) of the scattering profiles. At the beginning (0 min), the scattering profile showed a maximum at $q_{\max} = 0.44 \text{ nm}^{-1}$ indicating that the reactive blend was initially nanostructured. The location of this maximum is related to the average distance among nano-objects, in this case 15.7 nm ($2\pi/q_{\max}$). As reaction progressed, the maximum vanished and finally disappeared at 75 min of reaction, where a plateau at low- q range was observed. This behaviour can be ascribed to a partial coalescence among nanostructures, which resulted in a decrease in the number of micelles accompanied by an increase in their separation, giving place to a population of non-interacting spherical micelles. As reaction advanced, the slope of the SAXS curve below 0.3 nm^{-1} (Fig. 4b) showed a progressive decline from 0 to -1 close to 105 min, and then to -2 near 145 min. According to theory, a low- q slope of -1 in the Guinier regime could be assigned to rigid rods, whereas a slope of -2 could result from the presence of vesicles.⁵¹ From 145 min to the end of reaction, SAXS diagrams did not significantly changed indicating that the vesicles are probably the equilibrium morphology at high conversion values.



(a)



(b)

Figure 4. *In situ* SAXS data obtained during photo-polymerization at room temperature of the sample with 10 wt % PEB-*b*-PEO. (a) Full set of recorded SAXS curves recorded, and (b) SAXS curves at selected times of reaction.

Based on the obtained results from the Guinier analysis, which are in agreement with the commonly observed sequence of morphologies (i.e. sphere-to-cylinder-to-

vesicle) derived from the increasing segregation strength between the BCP and the epoxy matrix as polymerization progresses, we analyzed the SAXS data using the SASfit software package in the q -region from 0.1 to 0.7 nm⁻¹. Figure 5 shows the fitting of the SAXS data for selected times of reaction (See Supporting Information for a brief description of the model and the fitting results, Section S-3). Data obtained at 75 and 95 min were modeled assuming a population of polydisperse spherical micelles with a mean diameter of 11.1 and 14.4 nm respectively. On the other hand, data at 105 min of reaction required to assume a population of polydisperse rods with a mean diameter of 8.0 nm and length equal to 40.0 nm. The rod-to-vesicle transition was detected approximately at 135 min where a mixed population of rods and vesicles had to be introduced. From 145 min onward, data were modeled assuming only a population of polydisperse vesicles with an overall mean diameter of 49.2, 51.0 and 50.0 nm corresponding to 145, 195 and 235 min of reaction, respectively. For all these cases, the wall thickness corresponding to the bilayer membrane remained constant in approximately 13.0 nm. The analysis of SAXS data evidenced that during the first 100 min of reaction the system tends to reduce the total interfacial area by increasing the micellar size while reducing the total number of micelles. As reaction progresses, the spherical micelles convert into cylindrical micelles of a smaller diameter, thus reducing the total free energy of the system. As polymerization further proceeds, an analogous tendency to reduce the total free energy of the system forces a cylinder-to-vesicle transformation. Figure 6 shows a schematic representation of the morphological transformation that takes place during the room temperature photopolymerization for the sample with 10 wt % of BCP.

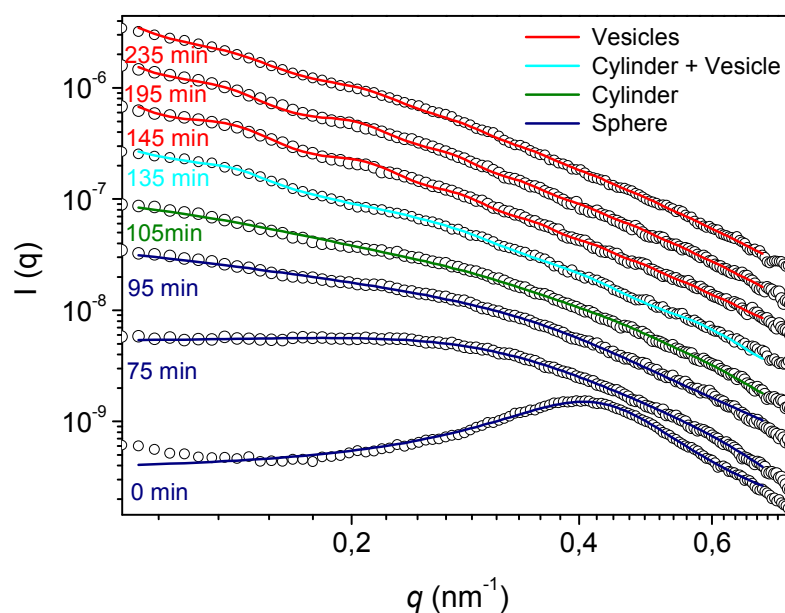


Figure 5. Fitting of SAXS data obtained at selected reaction times during the room temperature photo-polymerization of the sample with 10 wt% PEB-*b*-PEO.

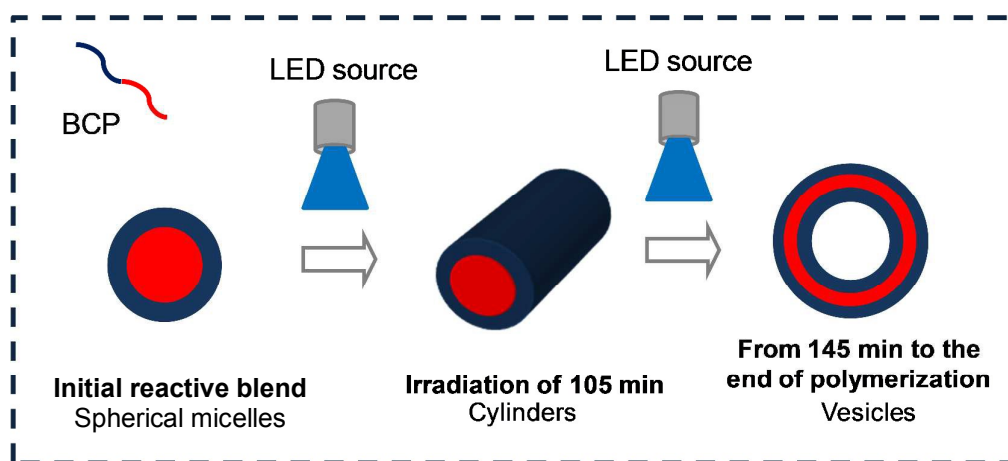


Figure 6. Schematic representation of the morphological transformation that takes place during the room temperature photopolymerization of the sample containing 10 wt% PEB-*b*-PEO.

In the literature, sphere-to-cylindrical-to-vesicle transformation of self-assembled structures have been observed under different conditions: (a) increasing the length of the hydrophobic block of the BCP in water solutions,²⁵⁻⁵² (b) varying the

solvent selectivity for one of the blocks,⁵ (c) increasing the fraction of water in water/organic solvent mixtures,^{3,5,53} and (d) increasing the concentration of BCP.⁵⁴ A sphere-to-cylinder-to-vesicle transformation was also reported in epoxy matrices by changing the BCP composition (i.e. decreasing the fraction of the epoxy-philic soluble block, in most of the cases a PEO block),^{4,18,20} keeping the same BCP composition but increasing its concentration in the blend,^{21,37} or increasing the molecular weight of the BCP.³⁶ In the present report, the morphological transition was triggered by the change in the quality of the epoxy solvent during polymerization. The epoxy monomer acts as a selective solvent for the PEO block producing a swollen “wet” PEO brush at the beginning of the reaction. During polymerization, the continuous increase in the size of epoxy oligomers decreases the miscibility of PEO through a reduction in the entropic contribution to the free energy of mixing. Under this circumstance, the polymerizing epoxy expels the PEO brushes creating conformational strains that induce a reduction of the local interfacial curvature. This is known as *wet to dry* brush transformation.⁴⁵

The arrest of the evolution of morphologies at about 145 min can be assigned to the gelation of the epoxy matrix. Although phase separation at a local level could still take place after gelation, generation of large vesicles must have occurred below this critical transition. The conversion at gelation obtained from the conversion vs. time curve of Fig. 2 is located at about 40 %. However, this value should be regarded with caution because the variation of geometries produced different irradiation intensities in both devices. A better value of the gel conversion was obtained by the rheometric characterization of samples irradiated for different times using a similar geometry as the one used to obtain the kinetic curve shown in Figure 2 (details are reported in the SI, Figure S-4). A cross-over of elastic and loss moduli was observed at a conversion close to 30 % which is a more reliable value of the gel conversion of our

particular formulation. Since curing was performed at room temperature, the polymerization rate was slow enough to allow full transition to occur prior to gelation. Vitrification causes restriction of mobility and sample hardening arresting any kind of nanoscale phase transition, as it was previously demonstrated.^{38,45} The vesicular morphology remained stable during a subsequent thermal postcuring of 1 hour at 120°C where the blend achieved full conversion, Figure S-5 (Supporting Information). A different situation occurred when curing was performed at 80 °C as will be discussed later.

To explore which intermediate structures were involved during the cylinder-to-vesicle transition, TEM images of a sample photocured for 120 min were taken. Figure 7 shows the coexistence of vesicles and cylinders as well as “jellyfish” like structures (marked with black circles in Figure 7). Jellyfish-like structures have been previously reported as important intermediates for the cylinder-to-vesicle transition. Essentially, the jellyfish-like hemispherical structure appears to be the final stage preceding vesicle formation.^{25,26,55,56}

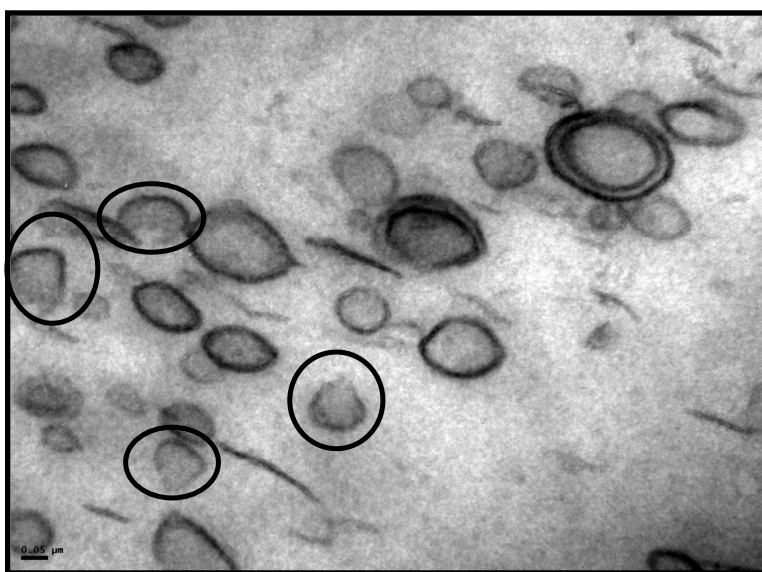


Figure 7. TEM image of a blend containing 10 wt% PEB-*b*-PEO irradiated for 120 min. The specimen was stained with RuO₄ prior to the TEM observation.

3.1.2. Curing at 80 °C. In this section we investigate the effect of increasing the curing temperature at 80 °C for the formulation with 10 wt% of PEB-*b*-PEO. In this case, the two-component photoinitiating system was replaced by BDMA as a thermal initiator of the epoxy homopolymerization.⁴² Figure 8 compares conversion vs. time curves for thermal cure at 80 °C and photocuring at room temperature. As can be seen, both curves were identical until a conversion value of approximately 0.1. After that point, the reaction rate at 80 °C accelerated with respect to room temperature, reaching the final conversion of photocuring (0.62) in only 2 h.

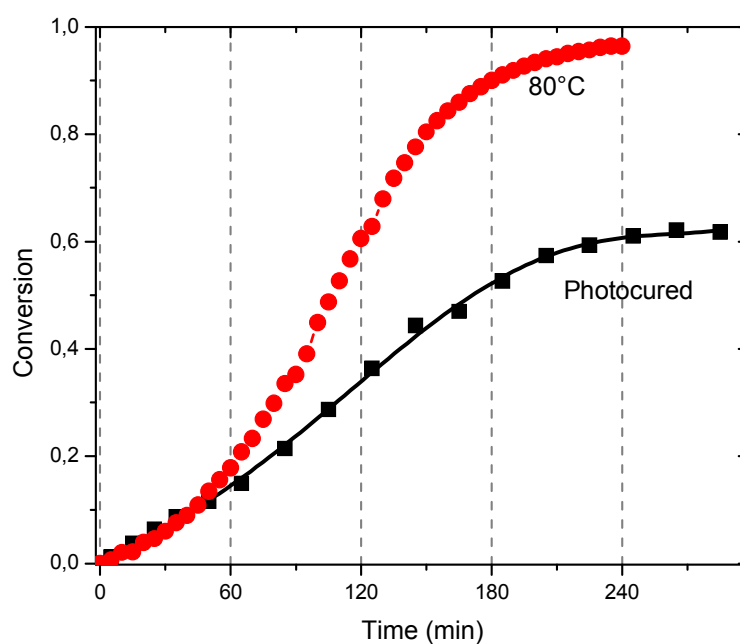


Figure 8. Conversion vs. time curves for the formulation with 10 wt% PEB-*b*-PEO, during thermal polymerization at 80 °C (circles) and photocuring at room temperature (squares).

Figure 9 shows TEM images of the sample containing 10 wt% of BCP cured at 80 °C. Surprisingly, spherical micelles partially arranged into micellar columns

coexisting with cylindrical micelles, were found instead of vesicles. This result indicates that the change in the reaction temperature had a direct effect on the developed morphology. To investigate how the morphology evolved during curing at 80 °C, *in situ* SAXS measurements were performed. As shown in Figure 10, the SAXS diagrams did not change significantly throughout the reaction. The only observed change was a shift of the position of the main peak towards lower q values, indicating an increase in the distance between nano-objects. The SAXS data, corresponding to 220 min (the last time acquired), was analyzed with the SASfit software assuming a population of polydisperse spherical and cylindrical micelles, with a structure factor introduced to account for the main peak. The mean spherical diameter obtained from the fitting procedure was 13 nm while the mean cylindrical diameter was 6 nm with a length of 13 nm. As Figure 10 shows, all the SAXS diagrams presented a slope of -4 in the high- q region (Porod regime). This indicates that the dispersing objects had smooth surface.^{51,57} It is evident that during cure at 80 °C a mixture of spherical and cylindrical structures was kinetically trapped by diffusion constraints imposed by the matrix polymerization.

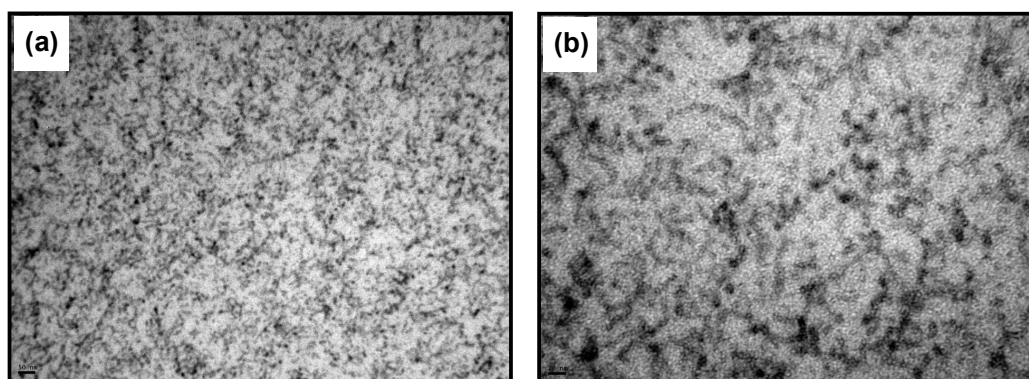


Figure 9. TEM images of the sample containing 10 wt% PEB-*b*-PEO fully cured at 80 °C. The specimen was stained with RuO₄ prior to the TEM observation. The black bar represents: a) 50 nm, and b) 20 nm.

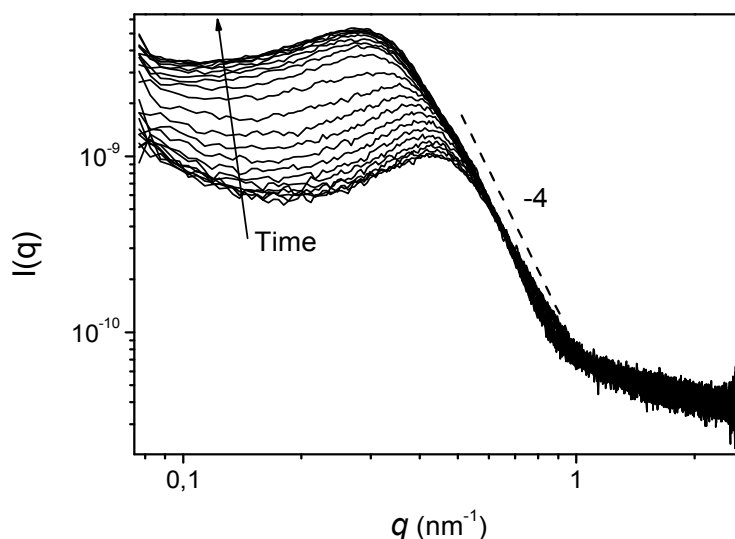


Figure 10. *In situ* SAXS diagrams obtained during polymerization of the sample with 10 wt% PEB-*b*-PEO at 80 °C.

3.2. Effect of the BCP concentration in the blend

It is well known that block copolymer vesicles are difficult to achieve, even more in thermosetting matrices.²¹ It has been demonstrated that vesicles can only be obtained within a very narrow concentration window. Therefore, the effect of the BCP concentration on the developed morphology is an important variable to be explored. With this aim in mind, we performed SAXS and TEM characterization of epoxy formulations containing 1, 20 and 40 wt % PEB-*b*-PEO photocured for 4 h at room temperature.

Figure 11 shows TEM micrographs at different magnification of a photocured sample with 1 wt% of BCP. The specimen was stained with RuO₄ prior to the TEM examination. Vesicular structures with bilayer wall are clearly observed with a mean diameter equal to 49.7 ± 13.1 nm (see histogram in the inset to Fig. 11a). Therefore, the

vesicles developed with 1 wt% BCP were similar to those obtained with 10 wt% BCP but with a smaller diameter.

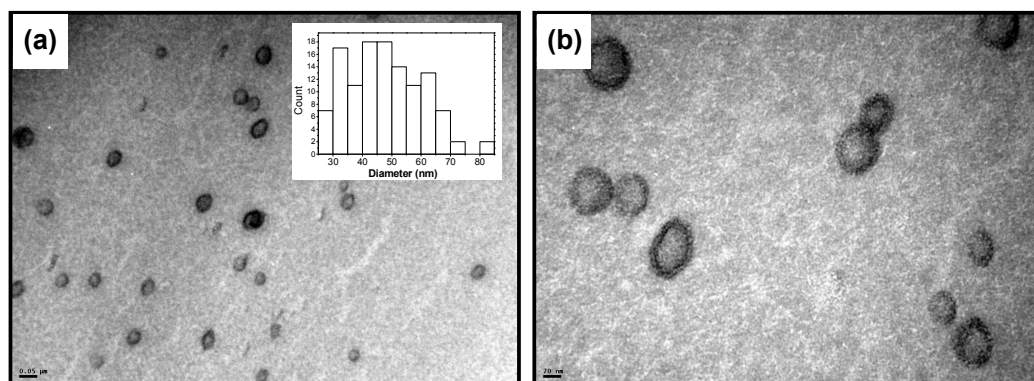


Figure 11. TEM images at different magnification of a photo-cured sample containing 1 wt% PEB-*b*-PEO. The specimen was stained with RuO₄ prior to the TEM observation. The black bar represents: a) 50 nm, and b) 20 nm.

Figure 12 shows TEM images of photocured samples with 20 and 40 wt% PEB-*b*-PEO. As can be observed, different morphologies were obtained by increasing the amount of BCP in the blend. For 20 wt% BCP (Fig. 12 a, b), the TEM images show unilamellar vesicles (i.e. bilayer vesicles) coexisting with multilayer vesicles. Upon close inspection of the multilayer vesicles (Fig. 12b), one can observe the presence of smaller unilamellar vesicles forming the different layers of the multilayer vesicles. In addition, partially fused multilayer vesicles can also be appreciated. Evidently, the morphologies captured by TEM correspond to a transient state, since, as is well known, membrane fusion in multivesicular systems results in the formation of multilayer vesicles.⁵⁸ Wang *et al.*⁵⁹ employed simulation of dynamic particles to investigate the self-assembly of graft copolymers in a backbone-selective solvent. They found that multilayer vesicles are formed through collision and fusion of unilamellar vesicles. In this way, multilayer vesicles continuously grow by increasing their number of layers. It should be noted that these intermediate multivesicular structures cannot be obtained

from phospholipids or other small-molecule surfactants due to their high mobility.⁶⁰ In our case, transient vesicular structures were captured because the curing reaction imposes diffusion constraints that prevent completion of the fusion processes involved in the structure evolution.

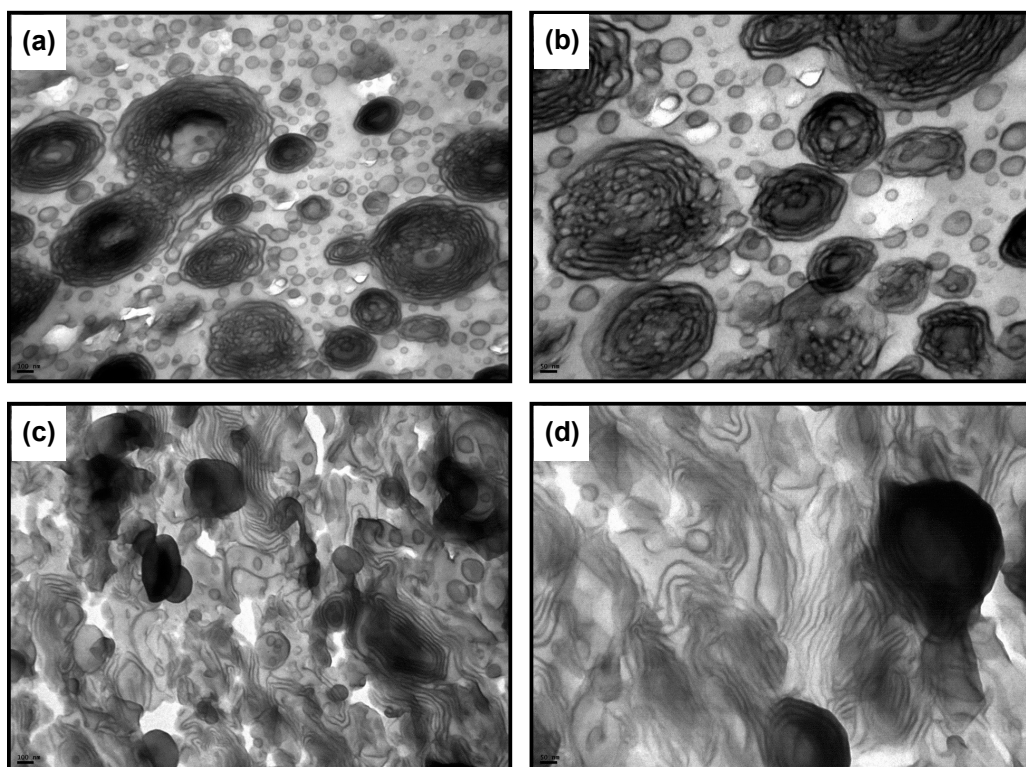


Figure 12. TEM images of the photocured samples containing: (a) 20 wt% PEB-*b*-PEO at lower magnification, (b) 20 wt% PEB-*b*-PEO at higher magnification, (c) 40 wt% PEB-*b*-PEO at lower magnification, (d) 40 wt% PEB-*b*-PEO at higher magnification. The specimens were stained with RuO₄ prior to the TEM observation.

For 40 wt% BCP (Fig. 12 c, d), the TEM images show a lamellar structure coexisting with multilayer vesicles. It should be noted that transient structures were not observed in this case, which would indicate that the system reached equilibrium morphology. This can be explained by the lower curing rate exhibited by the sample with 40 wt % BCP compared to the sample with 20 wt % BCP, see Supporting

Information (S-6). The rate of reaction is markedly reduced by the presence of 40 wt % BCP due to the contribution of several factors (as explained in 3.1.1). Hence the system has enough time and mobility to achieve equilibrium conditions.

SAXS measurements were carried out to extract complementary structural information. Figure 13 shows SAXS patterns for samples containing 20 and 40 wt % BCP. For both samples, the pattern presented a main peak accompanied by a higher order reflection located at $q_i/q^* = 2$ (indicated with arrows and better defined for the blend with 40 wt % BCP). Such a sequence is characteristic of a lamellar arrangement. For 20 wt% BCP, the main peak located at $q^* = 0.25 \text{ nm}^{-1}$, corresponds to an average interlamellar spacing of 25 nm. When the BCP concentration was increased from 20 to 40 wt%, the main peak slightly shifted to a higher q^* value, consistent with a decrease in the average interlamellar distance from 25 to 17 nm, respectively. At the same time, the main peak became more intense and sharper indicating that the stacking number and the organization of the layers increased with the BCP content, in agreement to what is seen in the TEM images.

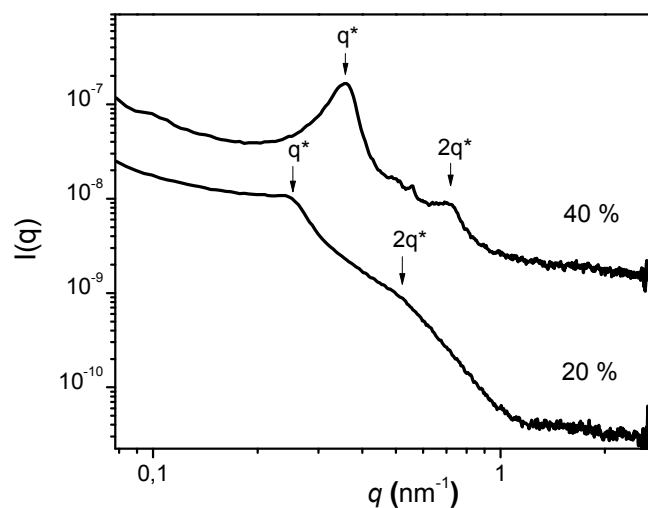


Figure 13. SAXS patterns of photocured samples containing 20 and 40 wt % PEB-*b*-PEO.

It has been well documented that for epoxy-based blends where vesicles are the stable morphology under dilute conditions, an increase in BCP concentration resulted in the formation of lamellae.¹⁹ On the other hand, Battaglia et al.⁶¹ investigated the phase diagram in the whole concentration range of poly(ethylene oxide)-*block*-poly(butylene oxide) BCP in water, and they found transitions from vesicles to packed/interconnected vesicles, then to a sponge-like phase and subsequently to lamellae by increasing the BCP concentration. Moreover, Braun et al.⁶² studied the binary phase diagram of poly(ethylene oxide)-*block*-poly(*g*-methyl- ϵ -caprolactone) BCP in water, and they found a transition from lamellae to packed vesicles and then to vesicles when the BCP concentration was decreased. In the present study, we demonstrated that bilayer vesicles can be obtained in the range between 1-10 wt% PEB-*b*-PEO via a sphere-to-cylinder-to-vesicle transition driven by the degree of polymerization of the epoxy matrix under photocuring conditions at room temperature. Under the same reaction conditions, the structure can evolve to multilayer vesicles or lamellae by increasing the BCP concentration up to 20 and 40 wt % respectively (Fig. 14).

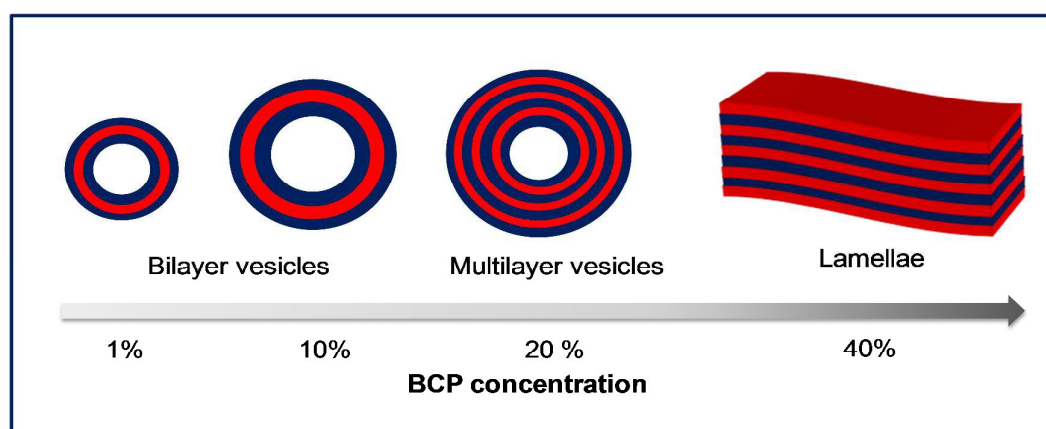


Figure 14. Schematic summary of the final morphologies obtained varying the BCP concentration.

4. CONCLUSIONS

The slow room temperature photopolymerization of a BCP/epoxy blend consisting of 1-10 wt% PEB-*b*-PEO dissolved in DGEBA monomer produced BCP vesicles dispersed in an epoxy matrix. *In-situ* SAXS measurements demonstrated that PEB-*b*-PEO was initially self-assembled into spherical micelles. During photocuring, a sphere-to-cylinder-to-vesicle transition took place driven by the tendency of the system to reduce the local interfacial curvature as a response to a decrease of the miscibility of PEO blocks in the polymerizing epoxy matrix. Under the same reaction conditions, the structure evolved to multilayer vesicles or lamellae by increasing the BCP concentration up to 20 and 40 wt% respectively. For 20 wt% BCP, transient structures, such as partially fused multilayered vesicles, were observed giving insight into the growth mechanism of multilayer vesicles. These transient structures were captured because the curing reaction imposed diffusion constraints that prevented completion of the fusion processes involved in the structure evolution. A formulation with 10 wt% BCP was also cured at 80 °C. Under these conditions, the polymerization reaction occurred at a faster rate and spherical micelles were kinetically trapped. Hopefully, this study will lead to new protocols for the preparation of vesicles dispersed in an epoxy matrix in a controlled way.

Conflicts of Interest

There are no conflicts of interest to declare.

ACKNOWLEDGEMENTS. The financial support of the following institutions is gratefully acknowledged: National Research Council (CONICET, Argentina), National Agency for the Promotion of Science and Technology (ANPCyT, Argentina),

University of Mar del Plata and Fundación Bunge y Born. The SAXS facility was acquired by a “Nanopymes” project, EuropeAid/132184/D/SUP/AR-Contract 331-896.

Author Contributions

The manuscript was written through contributions of all authors. All authors have given approval to the final version of the manuscript.

Supporting Information: **S-1:** DSC thermograms (at 10°C/min) of the neat BCP. **S-2:** SAXS measurements of the pristine epoxy resin before irradiation and after 240 min of irradiation. **S-3:** Brief description of the model and the fitting results of SAXS data obtained at selected reaction times during the room temperature photo-polymerization of the sample with 10 wt % PEB-*b*-PEO. **S-4:** Gel point determination by rheometric measurements. **S-5:** TEM image of sample containing 10 wt% PEB-*b*-PEO photocured 4h at room temperature and postcured 1h at 120°C. **S-6:** Conversion of epoxy groups as a function of irradiation time for blends containing 0, 10, 20 and 40 wt % PEB-*b*-PEO photocured at room temperature.

REFERENCES

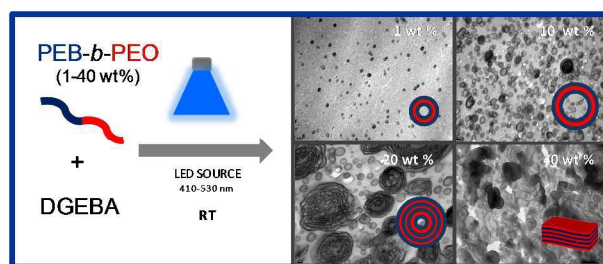
- 1 Y. Mai and A. Eisenberg, *Chem. Soc. Rev.*, 2012, **41**, 5969–5985.
- 2 R. C. Hayward and D. J. Pochan, *Macromolecules*, 2010, **43**, 3577–3584.
- 3 A. Choucair and A. Eisenberg, *Eur. Phys. J. E - Soft Matter*, 2003, **10**, 37–44.
- 4 J. Wu, Y. S. Thio and F. S. Bates, *J. Polym. Sci. Part B Polym. Phys.*, 2005, **43**, 1950–1965.
- 5 J. Bang, S. Jain, Z. Li, T. P. Lodge, J. S. Pedersen, E. Kesselman and Y. Talmon, *Macromolecules*, 2006, **39**, 1199–1208.
- 6 M. Karayianni and S. Pispas, in *Fluorescence Studies of Polymer Containing Systems*, ed. K. Procházka, Springer International Publishing, Cham, 2016, vol. 16, pp. 27–63.
- 7 Q. Liu, H. Zhu, J. Qin, H. Dong and J. Du, *Biomacromolecules*, 2014, **15**, 1586–1592.
- 8 T. Ren, Q. Liu, H. Lu, H. Liu, X. Zhang and J. Du, *J. Mater. Chem.*, 2012, **22**, 12329.
- 9 Y. Zhu, F. Wang, C. Zhang and J. Du, *ACS Nano*, 2014, **8**, 6644–6654.
- 10 M. Marguet, O. Sandre and S. Lecommandoux, *Langmuir*, 2012, **28**, 2035–2043.
- 11 X. Zhang, P. Tanner, A. Graff, C. G. Palivan and W. Meier, *J. Polym. Sci. Part Polym. Chem.*, 2012, **50**, 2293–2318.
- 12 Y. Zhu, L. Fan, B. Yang and J. Du, *ACS Nano*, 2014, **8**, 5022–5031.
- 13 D. L. Berthier, I. Schmidt, W. Fieber, C. Schatz, A. Furrer, K. Wong and S. Lecommandoux, *Langmuir*, 2010, **26**, 7953–7961.
- 14 Q. Geng and J. Du, *RSC Adv.*, 2014, **4**, 16425.
- 15 Q. Geng, J. Xiao, B. Yang, T. Wang and J. Du, *ACS Macro Lett.*, 2015, **4**, 511–515.

- 16 J. Hu, D. A. Koleva, P. Petrov and K. van Breugel, *Corros. Sci.*, 2012, **65**, 414–430.
- 17 L. Ruiz-Pérez, G. J. Royston, J. P. A. Fairclough and A. J. Ryan, *Polymer*, 2008, **49**, 4475–4488.
- 18 Y. S. Thio, J. Wu and F. S. Bates, *Macromolecules*, 2006, **39**, 7187–7189.
- 19 J. M. Dean, P. M. Lipic, R. B. Grubbs, R. F. Cook and F. S. Bates, *J. Polym. Sci. Part B Polym. Phys.*, 2001, **39**, 2996–3010.
- 20 J. M. Dean, R. B. Grubbs, W. Saad, R. F. Cook and F. S. Bates, *J. Polym. Sci. Part B Polym. Phys.*, 2003, **41**, 2444–2456.
- 21 Q. Guo, J. M. Dean, R. B. Grubbs and F. S. Bates, *J. Polym. Sci. Part B Polym. Phys.*, 2003, **41**, 1994–2003.
- 22 L. Luo and A. Eisenberg, *Langmuir*, 2001, **17**, 6804–6811.
- 23 M. J. Derry, L. A. Fielding, N. J. Warren, C. J. Mable, A. J. Smith, O. O. Mykhaylyk and S. P. Armes, *Chem. Sci.*, 2016, **7**, 5078–5090.
- 24 S. Sugihara, A. Blanz, S. P. Armes, A. J. Ryan and A. L. Lewis, *J. Am. Chem. Soc.*, 2011, **133**, 15707–15713.
- 25 A. Blanz, J. Madsen, G. Battaglia, A. J. Ryan and S. P. Armes, *J. Am. Chem. Soc.*, 2011, **133**, 16581–16587.
- 26 S. L. Canning, G. N. Smith and S. P. Armes, *Macromolecules*, 2016, **49**, 1985–2001.
- 27 J. Yeow, O. R. Sugita and C. Boyer, *ACS Macro Lett.*, 2016, **5**, 558–564.
- 28 J. Tan, C. Huang, D. Liu, X. Zhang, Y. Bai and L. Zhang, *ACS Macro Lett.*, 2016, **5**, 894–899.
- 29 Z. J. Thompson, M. A. Hillmyer, J. (Daniel) Liu, H.-J. Sue, M. Dettloff and F. S. Bates, *Macromolecules*, 2009, **42**, 2333–2335.
- 30 C. Ocampo, A. Tercjak, M. D. Martín, J. A. Ramos, M. Campo and I. Mondragon, *Macromolecules*, 2009, **42**, 6215–6224.
- 31 K. Bogaerts, A. Lavrenova, A. B. Spoelstra, N. Boyard and B. Goderis, *Soft Matter*, 2015, **11**, 6212–6222.
- 32 S. M. George, D. Puglia, J. M. Kenny, J. Parameswaranpillai, P. V. P. J. Pionteck and S. Thomas, *Phys. Chem. Chem. Phys.*, 2015, **17**, 12760–12770.
- 33 R. B. Grubbs, J. M. Dean, M. E. Broz and F. S. Bates, *Macromolecules*, 2000, **33**, 9522–9534.
- 34 L. Wang, C. Zhang, H. Cong, L. Li, S. Zheng, X. Li and J. Wang, *J. Phys. Chem. B*, 2013, **117**, 8256–8268.
- 35 H. Cong, L. Li and S. Zheng, *Polymer*, 2014, **55**, 1190–1201.
- 36 T. Li, M. J. Heinzer, L. F. Francis and F. S. Bates, *J. Polym. Sci. Part B Polym. Phys.*, 2016, **54**, 189–204.
- 37 R. Yu, S. Zheng, X. Li and J. Wang, *Macromolecules*, 2012, **45**, 9155–9168.
- 38 H. E. Romeo, I. A. Zucchi, M. Rico, C. E. Hoppe and R. J. J. Williams, *Macromolecules*, 2013, **46**, 4854–4861.
- 39 J. V. Crivello and K. Dietliker, *Photoinitiators for Free Radical Cationic & Anionic Photopolymerisation*, Wiley, 1999.
- 40 Y. Yagci, S. Jockusch and N. J. Turro, *Macromolecules*, 2010, **43**, 6245–6260.
- 41 Wiley, <http://www.wiley.com/WileyCDA/WileyTitle/productCd-3527332103.html>, (accessed November 2, 2016).
- 42 J. Puig, I. A. Zucchi, M. Ceolín, W. F. Schroeder and R. J. J. Williams, *RSC Adv*, 2016, **6**, 34903–34912.
- 43 A. Vazquez, D. Bentaleb and R. J. J. Williams, *J. Appl. Polym. Sci.*, 1991, **43**, 967–976.
- 44 N. Poisson, G. Lachenal and H. Sautereau, *Vib. Spectrosc.*, 1996, **12**, 237–247.
- 45 P. M. Lipic, F. S. Bates and M. A. Hillmyer, *J. Am. Chem. Soc.*, 1998, **120**, 8963–8970.
- 46 Y. Bi and D. C. Neckers, *Macromolecules*, 1994, **27**, 3683–3693.
- 47 J. V. Crivello and M. Sangermano, *J. Polym. Sci. Part Polym. Chem.*, 2001, **39**, 343–356.
- 48 I. A. Zucchi and W. F. Schroeder, *Polymer*, 2015, **56**, 300–308.
- 49 I. A. Zucchi, M. J. Galante and R. J. J. Williams, *Polymer*, 2005, **46**, 2603–2609.
- 50 S. Penczek, *J. Polym. Sci. Part Polym. Chem.*, 2000, **38**, 1919–1933.
- 51 O. Glatter and O. Kratky, *Small Angle X-ray Scattering*, Academic Press, 1982.

- 52 Y.-Y. Won, A. K. Brannan, H. T. Davis and F. S. Bates, *J. Phys. Chem. B*, 2002, **106**, 3354–3364.
- 53 N. Ali, W.-H. Sul, D.-Y. Lee, D.-H. Kim and S.-Y. Park, *Macromol. Res.*, 2009, **17**, 553–556.
- 54 P. Lim Soo and A. Eisenberg, *J. Polym. Sci. Part B Polym. Phys.*, 2004, **42**, 923–938.
- 55 N. J. Warren, O. O. Mykhaylyk, D. Mahmood, A. J. Ryan and S. P. Armes, *J. Am. Chem. Soc.*, 2014, **136**, 1023–1033.
- 56 D. Zehm, L. P. D. Ratcliffe and S. P. Armes, *Macromolecules*, 2013, **46**, 128–139.
- 57 J. S. Higgins and H. Benoît, *Polymers and neutron scattering*, Clarendon Press, 1994.
- 58 W. Yao, H. Qian, J. Zhang, W. Wu and X. Jiang, *Chem. Commun.*, 2012, **48**, 7079–7081.
- 59 L. Wang, T. Jiang and J. Lin, *RSC Adv.*, 2013, **3**, 19481.
- 60 J. A. Opsteen, J. J. L. M. Cornelissen and J. C. M. van Hest, *Pure Appl. Chem.*, , DOI:10.1351/pac200476071309.
- 61 G. Battaglia and A. J. Ryan, *Macromolecules*, 2006, **39**, 798–805.
- 62 J. Braun, N. Bruns, T. Pfohl and W. Meier, *Macromol. Chem. Phys.*, 2011, **212**, 1245–1254.

Controlling the generation of bilayer and multilayer vesicles in block copolymer / epoxy blends by a slow photopolymerization process

J. Puig,^a M. Ceolín,^b R. J. J. Williams,^a W. F. Schroeder,^a and I. A. Zucchi^{a,*}



Block copolymer vesicles were obtained in an epoxy matrix through a sphere>cylinder>vesicle morphological transition driven by slow photopolymerization at RT.